Water Oxidation and Oxygen Monitoring by Cobalt-Modified Fluorine-Doped Tin Oxide Electrodes

Caleb A. Kent,[†] Javier J. Concepcion,[†] Christopher J. Dares,[†] Daniel A. Torelli,[†] Adam J. Rieth,[‡] Andrew S. Miller,[‡] Paul G. Hoertz,[‡] and Thomas J. Meyer*,[†]

[†]Department of Chemistry, CB# 3290, University of North Carolina, Chapel Hill, North Carolina 27599, United States
[‡]RTI International, 3040 Cornwallis Road, Research Triangle Park, North Carolina 27709, United States

Ⓢ Supporting Information

ABSTRACT: Electrocatalytic water oxidation occurs at fluoride-doped tin oxide (FTO) electrodes that have been surface-modified by addition of Co(II). On the basis of X-ray photoelectron spectroscopy and transmission electron microscopy measurements, the active surface site appears to be a single site or small-molecule assembly bound as Co(II), with no evidence for cobalt oxide film or cluster formation. On the basis of cyclic voltammetry measurements, surface-bound Co(II) undergoes a pH-dependent $1e^-/1H^+$ oxidation to Co(III), which is followed by pH-dependent catalytic water oxidation. O_2 reduction at FTO occurs at −0.33 V vs NHE, allowing for in situ detection of oxygen as it is formed by water oxidation on the surface. Controlled-potential electrolysis at 1.61 V vs NHE at pH 7.2 resulted in sustained water oxidation catalysis at a current density of 0.16 mA/cm^2 with 29 000 turnovers per site over an electrolysis period of 2 h. The turnover frequency for oxygen production per Co site was 4 s^{-1} at an overpotential of 800 mV at pH 7.2. Initial experiments with Co(II) on a mesoporous, high-surface-area *nano*FTO electrode increased the current density by a factor of ∼5.

Water oxidation is an essential half-reaction in the formation of solar fuels by artificial photosynthesis.[1−3] In large-scale applications, first-row transition metal catalysts are desirable because of the quantities required at scale for global energy use. Cobalt oxide is a well-established water oxidation catalyst that first appeared in the patent literature in 1968.[4] It has recently been highlighted in electrocatalytic[5] and photoelectrochemical[6] applications by Nocera and co-workers. It is a relatively low-cost material with robust catalytic performance from pH 0 to 14.[7,8]

One approach to increasing the catalytic activity on a per-Co basis is to use nanostructured materials, in which the ratio of active to structural sites is increased.[9] We report here water oxidation catalysis by surface-bound Co on both planar fluoride-doped tin oxide (FTO) and high-surface-area *nano*-FTO electrodes. The underlying FTO conducting electrodes serve a dual role as a conductive support for Co-catalyzed water oxidation and as a sensor for O_2 as it is produced.

To prepare the electrodes, commercial 15 Ω FTO (Hartford) or 600 nm thick *nano*FTO composed of 100−300 nm particles [Keeling and Walker, Brunauer−Emmett−Teller (BET) specific surface area = 10−15 m^2/g] on a planar FTO

substrate was loaded with Co^{2+} by dipping 1−2 cm^2 of the slide in 1 mM Co(ClO$_4$)$_2$ in methanol for 1 h at room temperature. Loading with CoF$_2$ was also effective, but the perchlorate salt was more convenient because of its higher solubility. After Co^{2+} loading, the slides were thoroughly rinsed with methanol and water to remove any excess of salt and then dried for use in X-ray photoelectron spectroscopy (XPS) and transmission electron microscopy (TEM) measurements. The synthesis of *nano*FTO on planar FTO followed an earlier procedure for *nano*ITO.[10] *nano*FTO films were loaded in the same manner and washed by centrifugation with methanol and water. This approach differs from earlier procedures that utilized electrochemical deposition.[5,8]

A cyclic voltammogram (CV) of a Co-modified FTO electrode in aqueous 0.1 M phosphate with 0.5 M added NaClO$_4$ is shown in Figure 1a, and a plot of $E_{1/2}$ versus pH for
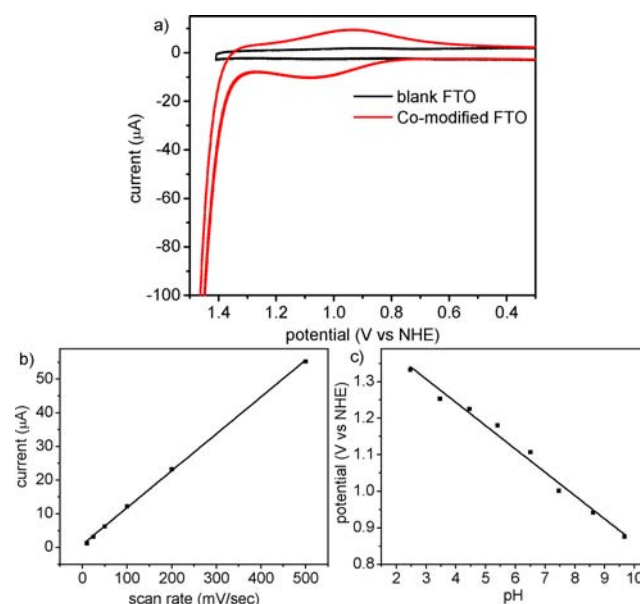
Figure 1. Electrochemical data for a Co(II)-modified planar FTO electrode. (a) CV in aqueous 0.1 M phosphate at pH 7.2 with 0.5 M added NaClO$_4$ at a scan rate of 100 mV/s. (b) Variation of the peak current with scan rate. (c) Variation of $E_{1/2}$ with pH. $E_{1/2}$ decreased by 64 mV per pH unit.

the reversible couple (see below) from pH 2−10 in appropriate buffers is presented in Figure 1c. In an oxidative scan at pH 7.2, a wave appeared at $E_{1/2}$ = 1.01 V vs NHE followed by the catalytic onset of water oxidation at ~1.3 V vs NHE. The peak current for the reversible wave varied linearly with scan rate (Figure 1b), consistent with a surface couple.[11] The process was pH-dependent, with $E_{1/2}$ decreasing by 64 mV/pH unit, which is close to the expected value of 59 mV/pH unit for a $1e^-/1H^+$ process, presumably the Co^{III}−OH/Co^{II}−OH_2 couple (Figure 1c).[11]

The same surface-loading strategy was explored for Mn^{2+} and Fe^{2+}. Loading FTO with $MnSO_4$ resulted in reversible oxidation waves at $E_{1/2}$ = 0.48 and 0.95 V vs NHE and a water oxidation onset at ~1.4 V vs NHE at pH 7.2 [Figure S1 in the Supporting Information (SI)]. With $FeSO_4$, there was no well-defined wave prior to the oxidation onset, which was also at ~1.4 V vs NHE (Figure S2).

The presence of Co(II) on FTO was confirmed by XPS. Earlier results on Co-doped SnO_2 showed that Co(II) replaces Sn(IV) in the FTO lattice, likely accompanied by formation of oxygen vacancies.[12] Co(II) and Co(III) have similar 2p binding energies but can be differentiated by the Co $2p_{1/2}$−$2p_{3/2}$ spin−orbit level energy spacing, which is 16.0 eV for high-spin Co(II) and 15.0 eV for low-spin Co(III).[13] The binding energies of Co on FTO were found to be 797.2 eV for Co $2p_{1/2}$ and 781.2 eV for Co $2p_{3/2}$, consistent with Co(II).

As shown in Figure 2, surface-bound Co(II) desorbed from SnO_2 at pH 7.2 following reductive scans past the reversible
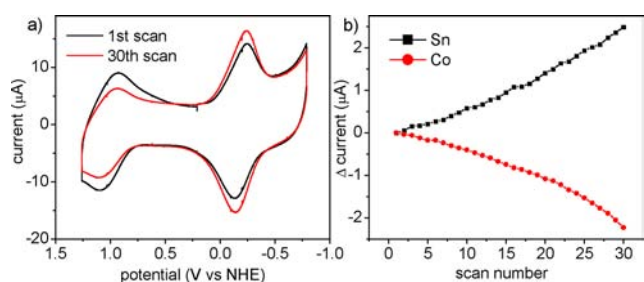
Figure 2. (a) Changes in current−potential waveforms with reductive scans for Co-modified FTO in 0.1 M phosphate at pH 7.2 with 0.5 M added NaClO₄ at a scan rate of 100 mV/s. (b) Peak currents at −0.19 V vs NHE [Sn(IV) reduction] and 1.01 V vs NHE [Co(II) oxidation] plotted for 30 scans, illustrating Co(II) loss.

Sn(IV)/Sn(II) wave at $E_{1/2}$ = −0.19 V vs NHE.[14,15] The peak current for Sn(IV) reduction increased with the number of scans, accompanied by a decrease in the peak current for the Co(III)/Co(II) wave at $E_{1/2}$ = 1.01 V vs NHE. The Co(III)/Co(II) wave was stable indefinitely in oxidative scans.

The available evidence points to water oxidation by single-site catalysis at surface sites occupied by Co(II). Water oxidation by ~1 nm diameter cobalt oxide clusters on silica nanoparticles has been observed,[16] but there was no evidence for cluster formation on FTO in TEM measurements (Figure S4). The surface coverage was submonolayer, as determined by integration of the current−potential waveforms in the CV measurements. If it is assumed that the radius of Co units on the surface is 3.3 Å, as for $Co(H_2O)_6^{2+}$ on the basis of molecular modeling, a maximum random close-packed surface coverage of 3.1×10^{-10} mol/cm² is obtained. With n = 1 for the Co(II) oxidation wave at $E_{1/2}$ = 1.01 V vs NHE at pH 7.2, a surface coverage of 7.0×10^{-11} mol/cm² (i.e., 20−25% of the

theoretical maximum loading) was obtained after a 1 h soaking period. There was some variation in loading among the samples, but the extent of loading was not enhanced by increasing the soaking time.

To confirm that the observed catalysis is distinct from the water oxidation catalysis by the phosphate- and borate-containing cobaltate clusters reported by Nocera and co-workers,[5,6] water oxidation electrolysis was carried out at 1.6 V vs NHE in an aqueous carbonate buffer at pH 6.7 at an ionic strength of 0.1 M with no added phosphate (Figure S9). After passage of 1 C, CV scans showed that the surface Co(III)/Co(II) wave remained essentially unchanged (Figure S10). The slide was then removed, rinsed with methanol, dried, and examined by XPS, atomic force microscopy (AFM), and scanning electron microscopy (SEM). XPS confirmed the presence of Co(II) rather than Co(III) as observed by Nocera and co-workers. AFM and SEM measurements revealed unchanged surfaces with no evidence for cluster formation. Electrolyses under the same conditions in an aqueous phosphate buffer at pH 7.2 gave the same results, with no evidence for surface cluster formation. A series of controlled-potential electrolyses were carried out at 1.6 V vs NHE in both carbonate (pH 6.7, I = 0.1) and phosphate (pH 7.2, I = 0.1) buffers with added $Co(ClO_4)_2$. There is evidence of film formation in carbonate buffer with free Co^{2+} in solution; however, the film (likely a type of cobaltate) does not enhance the electrocatalysis. In the phosphate buffer, the CoPi film described by Nocera and co-workers was formed, as shown by CV measurements (Figure S13).[5] Removal of the film by rinsing the electrode with 1 M perchloric acid regenerated the initial CV for the Co-modified electrode (Figure S13).

FTO electrodes are known to be active toward oxygen reduction. In CVs under an air and or oxygen atmosphere (Figure S6), a broad O_2 reduction wave at −0.3 to −0.4 V vs NHE appeared.[15] The ability of FTO to sense oxygen and, on derivatized surfaces, to support water oxidation catalysis allows it to act as its own internal probe for analyzing O_2 as it forms. In situ O_2 sensing was demonstrated for the well-characterized water oxidation catalyst $[Ru(mebimpy)(bpy)(OH_2)]^{2+}$ [mebimpy = 2,6-bis(benzimidazol-2-yl)pyridine; bpy = 2,2'-bipyridine] (Figure 3a).[17] In an argon-deaerated solution of the catalyst at pH 7.2 in a 0.1 M phosphate buffer, water oxidation was initiated at an onset potential of ~1.5 V vs NHE following oxidation of $[Ru^{IV}(mebimpy)(bpy)(O)]^{2+}$ to $[Ru^{V}(mebimpy)(bpy)(O)]^{3+}$. As can be seen in Figure 3a, experiments involving potential holds at 1.81 V vs NHE for various times followed by reductive scans past the Sn(IV)/Sn(II) wave at $E_{1/2}$ = −0.19 V vs NHE provided direct evidence for O_2 formation by the enhanced current for O_2 reduction at $E_{p,c}$ = −0.33 V vs NHE.

As shown in Figure 3b, the same effect was observed on Co(II)-modified FTO with the electrode acting as its own O_2 sensor. Oxidative scans to 1.61 V vs NHE produced O_2, as demonstrated by the increase in the reductive peak current at −0.33 V vs NHE on the return reductive scan.

As shown in the Tafel plots in Figure S7, the catalytic current density varied logarithmically with overpotential, with slopes of ~80 mV per decade over the pH range 4.5−8.0. Although the pH effect remains to be studied in detail, its appearance is consistent with an observation made for water oxidation by $[Ru(mebimpy)(bpy)(OH_2)]^{2+}$. For this complex, rate accelerations were observed with added base ($H_2PO_4^-$, acetate, or HPO_4^{2-}) and attributed to the intervention of "atom−proton
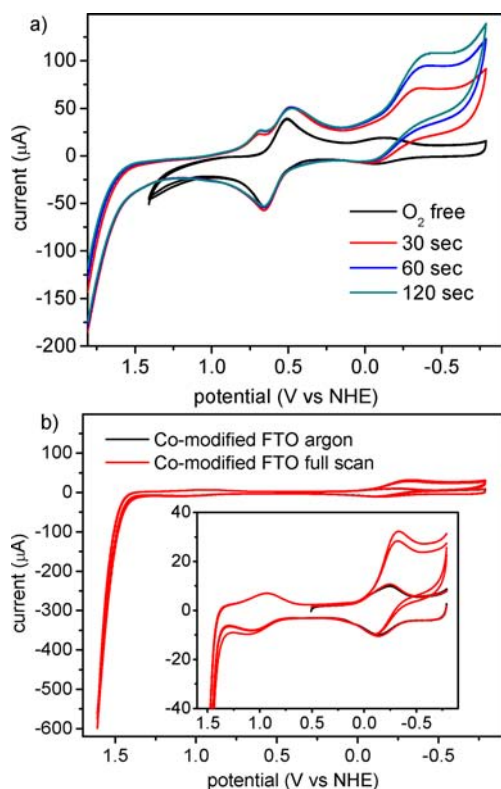
Figure 3. (a) CVs of 1 mM $[Ru(mebimpy)(bpy)(OH_2)]^{2+}$ in argon-deaerated 0.1 M phosphate buffer at pH 7.2 at 100 mV/s on FTO. The potential was held at 1.81 V vs NHE for either 30 (red), 60 (blue), or 120 s (green) prior to the reductive scan. (b) CV scans of Co-modified FTO under argon following oxidative scans to 1.61 V vs NHE at 100 mV/s, showing the appearance of the O_2 reduction wave at $E_{p,c} = -0.33$ V vs NHE.

transfer" (APT) involving O−O bond formation assisted by concerted loss of a proton to the added buffer base:[18]

$$Ru^V(O)^{3+} + HO-H\cdots HPO_4^{2-} \rightarrow Ru^{III}-OOH^{2+} + H_2PO_4^-$$
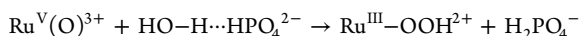
On the basis of steady-state current measurements at an applied potential of 1.61 V vs NHE at pH 7.2 (Figure 4a), the
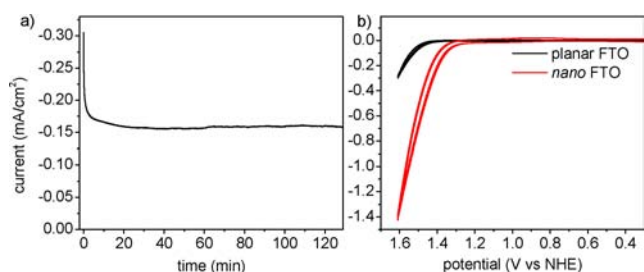
Figure 4. (a) Controlled-potential electrolysis of Co-modified planar FTO at 1.61 V vs NHE. (b) CVs of Co-modified planar and *nano*FTO electrodes in 0.1 M phosphate buffer at pH 7.2 with 0.5 M added $NaClO_4$.

turnover frequency for water oxidation by Co on FTO (see the SI for details) is 4 s^{-1} at an overpotential of 800 mV. Literature values reported for cobalt oxide clusters on a per Co basis range from ≥0.0007[5] to 0.035 s^{-1},[19] but these were found at different overpotentials and are not directly comparable.[9]

To achieve current densities that are useful at scale, much higher Co loading levels are required. We initiated a series of

experiments with high-surface-area conducting *nano*FTO electrodes.[5] Initial results were obtained with a 600 nm thick *nano*FTO film prepared from 100−300 nm nanoparticle precursors and derivatized with Co(II) by soaking in a methanol solution of $Co(ClO_4)_2$. As shown in Figure 4b, the current density was enhanced by a factor of ∼5 relative to planar FTO. Strategies for further enhancement of the effective surface coverage of Co(II) on *nano*FTO are currently under investigation.[6]

The results described here are important in adding to growing insights on water oxidation catalysis by first-row transition metals. The evidence for Co-modified FTO suggests surface binding as Co(II), which, following oxidation to Co(III) and proton loss, undergoes further oxidation, triggering water oxidation catalysis. The water oxidation rate was 4 s^{-1} per Co site in pH 7.2 water at 1.61 V, and from the controlled-potential electrolysis results in Figure 4, turnover numbers of 28 000 per Co site were achieved over a 2 h electrolysis period with no sign of loss of catalytic activity. Higher rates were achieved on high-surface-area *nano*FTO.

The strategy adopted here, involving surface loading of a limited number of Co(II) sites on conducting, high-surface-area, porous FTO electrodes, allows for a significant decrease in Co content compared with cobalt oxide films or clusters while achieving high current densities. This is no doubt due in part to maximization of the number of catalytically active sites, in contrast to cobalt oxide clusters, where the interior Co sites presumably function only to support the structure and promote electron transport to active sites on the surface. The FTO electrodes have the additional advantage of acting as internal O_2 sensors by electrochemical monitoring.

■ ASSOCIATED CONTENT

Ⓢ Supporting Information

Experimental procedures and characterization data. This material is available free of charge via the Internet at http://pubs.acs.org.

■ AUTHOR INFORMATION

Corresponding Author

tjmeyer@unc.edu

Notes

The authors declare no competing financial interest.

■ ACKNOWLEDGMENTS

■ REFERENCES

(1) Alstrum-Acevedo, J. H.; Brennaman, M. K.; Meyer, T. J. *Inorg. Chem.* **2005**, *44*, 6802.

(2) Concepcion, J. J.; Jurss, J. W.; Brennaman, M. K.; Hoertz, P. G.; Patrocinio, A. O. T.; Murakami, I. N. Y.; Templeton, J. L.; Meyer, T. J. *Acc. Chem. Res.* **2009**, *42*, 1954.

(3) Lewis, N. S.; Nocera, D. G. *Proc. Natl. Acad. Sci. U.S.A.* **2006**, *103*, 15729.

8434

dx.doi.org/10.1021/ja400616a | *J. Am. Chem. Soc.* 2013, 135, 8432−8435

(4) Suzuki, O.; Takahashi, M.; Fukunaga, T.; Kuboyama, J. (Tsurumi Soda Co., Ltd.). U.S. Patent 3,399,966, Sept 3, 1968.

(5) Kanan, M. W.; Nocera, D. G. *Science* **2008**, *321*, 1072.

(6) Reece, S. Y.; Hamel, J. A.; Sung, K.; Jarvi, T. D.; Esswein, A. J.; Pijpers, J. J. H.; Nocera, D. G. *Science* **2011**, *334*, 645.

(7) Gerken, J. B.; Landis, E. C.; Hamers, R. J.; Stahl, S. S. *ChemSusChem* **2010**, *3*, 1176.

(8) Gerken, J. B.; McAlpin, J. G.; Chen, J. Y. C.; Rigsby, M. L.; Casey, W. H.; Britt, R. D.; Stahl, S. S. *J. Am. Chem. Soc.* **2011**, *133*, 14431.

(9) Jiao, F.; Frei, H. *Energy Environ. Sci.* **2010**, *3*, 1018.

(10) Hoertz, P. G.; Chen, Z.; Kent, C. A.; Meyer, T. J. *Inorg. Chem.* **2010**, *49*, 8179.

(11) Bard, A. J.; Faulkner, L. R. *Electrochemical Methods: Fundamentals and Applications*, 2nd ed.; Wiley: New York, 2001.

(12) Batzill, M.; Burst, J. M.; Diebold, U. *Thin Solid Films* **2005**, *484*, 132.

(13) Oku, M.; Hirokawa, K. *J. Electron Spectrosc. Relat. Phenom.* **1976**, *8*, 475.

(14) Batzill, M.; Diebold, U. *Prog. Surf. Sci.* **2005**, *79*, 47.

(15) Ichinose, K.; Kimikado, Y.; Yoshida, T. *Electrochemistry (Tokyo, Jpn.)* **2011**, *79*, 146.

(16) Zidki, T.; Zhang, L.; Shafirovich, V.; Lymar, S. V. *J. Am. Chem. Soc.* **2012**, *134*, 14275.

(17) Concepcion, J. J.; Tsai, M.-K.; Muckerman, J. T.; Meyer, T. J. *J. Am. Chem. Soc.* **2010**, *132*, 1545.

(18) Chen, Z.; Concepcion, J. J.; Hu, X.; Yang, W.; Hoertz, P. G.; Meyer, T. J. *Proc. Natl. Acad. Sci. U.S.A.* **2010**, *107*, 7225.

(19) Harriman, A.; Pickering, I. J.; Thomas, J. M.; Christensen, P. A. *J. Chem. Soc., Faraday Trans. 1* **1988**, *84*, 2795.